Zohreh Alemansour and Mehdi Zarei. Combined use of hydrogeological, hydrogeochemical and isotopic techniques to identify the impact of a salt diapir on surrounding aquifers, Southern Iran. *Journal of Cave and Karst Studies*, v. 81, no. 3, p. 203-215. DOI:10.4311/2018ES0120

COMBINED USE OF HYDROGEOLOGICAL, HYDROGEOCHEMICAL AND ISOTOPIC TECHNIQUES TO IDENTIFY THE IMPACT OF A SALT DIAPIR ON SURROUNDING AQUIFERS, SOUTHERN IRAN

Zohreh Alemansour and Mehdi Zarei[1]

Abstract

More than 120 exposed salt diapirs in southern Iran are connected to the adjacent aquifers and likely constitute the main sources of groundwater salinization in the region. Located in southern Iran, the Korsia salt diapir is surrounded by alluvial and karst groundwater aquifers. To investigate the impact of the salt body of Korsia on the groundwater quality of surrounding aquifers, electrical conductivity, total dissolved solids and dissolved calcium, magnesium, sodium, potassium, chloride, bromide, and sulfate concentrations were measured at 41 sampling points, including 32 exploitation wells, 7 springs and 2 surface water stations. Additionally, oxygen-18 and deuterium isotopes were analyzed at 7 sampling points to investigate the source of the salinity in the area. Our hydrogeological, hydrogeochemical, and isotopic evaluations show that the Korsia diapir deteriorates groundwater quality of the eastern karst and southern alluvial aquifers through infiltration of a spring's brine into limestone, and flow of the surface brine originated from the diapir, respectively. A karst aquifer west of the diapir is not influenced by the diapir brine because its hydraulic connectivity is interrupted by an impermeable geological formation. Construction of salt basins or diversion of brine is suggested to increase water quality of the surrounding aquifers. These procedures can be applied not only in the Korsia diapir, but also in tens of diapirs of southern Iran as remediation methods to improve water quality of their adjacent aquifers in this arid region.

Introduction

There are more than 120 emerged salt diapirs in the Zagros Mountain Ranges of southern Iran (Talbot and Alavi, 1996; Bosák et al., 1999; FDA, 2016; Zarei, 2016). Intrusion of brines from these salt diapirs into their surrounding water resources contributes to degrade the quality of surface and underground waters of southern Iran (Zarei, 2010; Zarei et al., 2014). Salt diapirs are also reported in the United States (the Gulf Coast region and southeast Utah), the Dead Sea coasts, the northern German Plain, and northeast Spain (Frumkin, 1994; Bosák, 1999; Kloppmann et al., 2001; Hamlin, 2006; Lucha et al., 2008). Investigations dealing with exposed salt diapirs in Spain and the Dead Sea coasts have been mainly the subject of salt speleogenetic studies, whereas their impact on water quality on the surrounding water resources have not been considered so far. The salt diapirs in the United States (Hamlin, 2006) and Northern Germany (Kloppmann et al., 2001) have no exposure at the surface and their effect on water quality has been evaluated in detail.

Geomorphological and hydrogeological aspects of salt diapirs of southern Iran have been studied in detail by several investigators over the last two decades. Bruthans et al. (2000) characterized the factors affecting morphogenesis of salt karst in southern Iran, pointing to thickness of caprock as a major factor that influences superficial and underground karst forms. The most important factors affected by caprock thickness are, in turn, the density of recharge points, the amounts of concentrated recharge, the rate of ground surface lowering, the dissolution capacity of water, and the size and amount of load transported by underground flood-streams into cave systems. Bruthans et al. (2006) estimated the age, depositional history and uplift rates of marine terraces of the Hormoz and Namakdan salt diapir in the Persian Gulf, based on radiocarbon dating. The erosion rates of residuum and rock salt exposures on several salt diapirs with different climatic settings were measured in southern Iran for a period of five years by Bruthans et al. (2008). They found that denudation of rock salt exposures is much faster than the diapirs covered by weathering residuum. Bruthans et al. (2009) studied surficial deposits of 11 Iranian salt diapirs, and characterized that the source material, diapir relief, climatic conditions, and vegetation cover were the main factors affecting the development and erosion of surficial deposits. Evolution of salt diapir and karst morphology of the coastal salt diapir of Namakdan, southern Iran, were evaluated based on known sea-level oscillations, radiometric dating, and geological evidence (Bruthans et al., 2010).

Comparing the evolution of Namakdan diapir with the Hormoz and Larak diapirs, they showed that the evolution of diapir morphology is strongly affected by the differences in uplift rates and geological settings. Bruthans et al. (2017) studied soil, drip, stream, and flood waters from different environments at several diapirs of southern Iran, and they found that the soil water chemistry depends on both the climate and cap soil thickness. Abirifard et al. (2018) studied model of flow direction and hydrochemical effects of the Jahani salt diapir on the adjacent water. They also characterized the major factors controlling the morphological aspects of salt karst at the Jahani diapir.

[1] Department of Earth Sciences, Shiraz University, Shiraz, Iran. Corresponding author: zareim@shirazu.ac.ir

A variety of chemical constituents and ratios have been suggested to distinguish halite-solution brine from other potential sources of salinization, such as evaporation of groundwater (Richter et al., 1991; Kloppmann et al., 2001; Davidson and Mace, 2006; Jirsa et al., 2013; Ying et al., 2013; Kumar, 2014; Salameh et al., 2014; Lichun Ma et al., 2016; Ebrahimi et al., 2016;). Intrusion of halite-solution brines typically produces significant changes in groundwater chemistry from more Ca-HCO_3 to Na-Cl type (Kreitler and Richter, 1986). The molar ratio of Na/Cl has been also suggested by Leonard and Ward (1962) to characterize halite-solution brines. Sodium (Na) and chloride (Cl) are present in halite at equal molar concentrations, and therefore, the Na/Cl molar ratio is close to one in brines that originate from salt diapirs (Richter et al., 1990). Bromide is extensively used in combination with chloride as a useful tracer in the study of saline waters (Richter et al., 1991; Cartwright et al., 2006; Zarei, 2010; Charef, et al., 2012). Both constituents (Br and Cl) are conservative and they are not easily removed by processes such as ion exchange or precipitation)Kreitler and Richter, 1986). Their ratio (Br/Cl) can be used as a tracer of salinization sources. The Br/Cl ratio in brines related to halite dissolution (Br/Cl $<4 \times 10^{-4}$) is typically one order of magnitude smaller than in other water sources. Many authors have applied Br/Cl ratio in their studies to identify sources of salinization, including Whittemore and Pollock (1979), Kreitler and Richter (1986), Morton (1986), Kreitler (1993) and Kharroubi et al. (2012).

The water quality of alluvial and karst aquifers surrounding the salt diapirs of southern Iran are typically deteriorated by intrusion of diapir-derived brine, and this represents one of the main hydrogeological problems affecting karst aquifers in Iran (Karimi and Taheri, 2010; Taheri et al., 2016, 2017). Zarei (2016) evaluated 62 salt diapirs in southern Iran to identify factors governing the impact of salt diapirs on the surrounding water resources. The author concluded that the main controlling factors are: i) the evolutionary stage of the diapirs, ii) the geology, iii) the hydrogeological setting, and iv) the anthropogenic activities. Moreover, Mehdizadeh et al. (2015) studied how the 62 salt diapirs of southern Iran influence water quality in the surrounding aquifers, reporting that the main mechanisms of the adjacent aquifers' deterioration are related to: a) diapir-brine intrusion in the subsurface, b) re-infiltration of brine emerging from springs, and c) infiltration of saline runoff originating from the surface of the diapirs. The effects of several, individual salt diapirs on adjacent aquifers in southern Iran have been also evaluated at the Konarsiah diapir (Sharafi et al., 1996; Zarei and Raeisi, 2010; Zarei et al., 2013), Gaztavileh diapir (Sharafi et al., 2002), Bastak diapir (Zarei et al., 2014), and Karmustadje diapir (Nekouei and Zarei, 2016). For instance, Sharafi et al. (2002) studied the impact of the Gaztavileh salt diapir on the adjacent karst aquifer and reported that the water quality is degraded by the diapir brine. Nekouei et al. (2016) evaluated the influence of Karmustadj salt diapir on aquifers using hydrogeochemical and isotopic techniques. They found that diapir-derived brines intrude the surrounding alluvial aquifers but have no degrading impact on the adjoining karst aquifer.

Salt has a particularly low-yield strength, and consequently, is subject to plastic deformation under differential pressure (Anderson and Brown, 1992). The role of halokinesis in salt karst hydrology has been evaluated by some researchers. Frumkin (2000) studied how halokinesis inhibit deep development of salt caves in salt diapirs of the Dead Sea area. Chiesi et al. (2010) related the sudden increase in salinity of springing waters in Poiano area, Italy, to active halokinesis causing new bodies of rock salt to reach the water table (De Waele et al., 2017).

The Korsia salt diapir of southern Iran is in direct contact with adjacent karst and alluvial aquifers, and in addition, shows several brine springs that emerge from the diapir. The surrounding wells and springs are characterized by fresh to brackish waters. The overall purposes of this study are to: i) evaluate the salinity distribution of waters in the Korsia area, ii) demonstrate that the salt diapir is the main source of aquifer salinization, and iii) describe how this diapir influences water quality.

Geological, Geomorphological and Hydrogeological Setting

The salt diapir of Korsia is located in south-central Iran, 15 km west from the city of Darab (Fig. 1). The diapir occurs on the southern limb of the Shahneshin Anticline, situated in the Zagros Mountains. The Shahneshin Anticline follows the general NW-SE trend of the Zagros. James and Wynd (1965) and Falcon (1974) described the stratigraphical and structural characteristics of the Zagros sedimentary sequence. The exposed geological formations of the study area, from the oldest to the youngest, include Hormuz salts (Precambrian-Middle Cambrian), Sarvak limestones (Cretaceous), Radiolarite Unit (Cretaceous), Tarbur limestones (Upper Cretaceous), Sachun marlstones (Upper Cretaceous- Paleocene), Jahrum limestones and dolostones (Oligocene), Razak shales and marlstones (Oligo-Miocene), and Gachsaran marls and evaporites (Tertiary). The bedrock is unconformably overlain by Quaternary alluvium that characterizes the alluvial plain (Falcon, 1967; Berberian and King, 1981; Alavi, 2004). The salt rocks of Korsia diapir belong to the Hormuz Formation with an approximate original thickness of 1 km (Stöcklin, 1968; Kent, 1979).

The Korsia salt diapir has an elliptical shape with an area of 2.64 km^2 (Fig. 2a). Mehdizadeh et al. (2015) characterized it as an active diapir in terms of the evolutionary stages of salt diapirs. An active salt diapir has a positive relief with significant area of salt rock exposures. Table 1 summarizes the morphological characteristics of the Korsia diaper, the maximum length and width of the diapir being 2.40 and 1.48 km, respectively. The maximum elevation of the diapir is

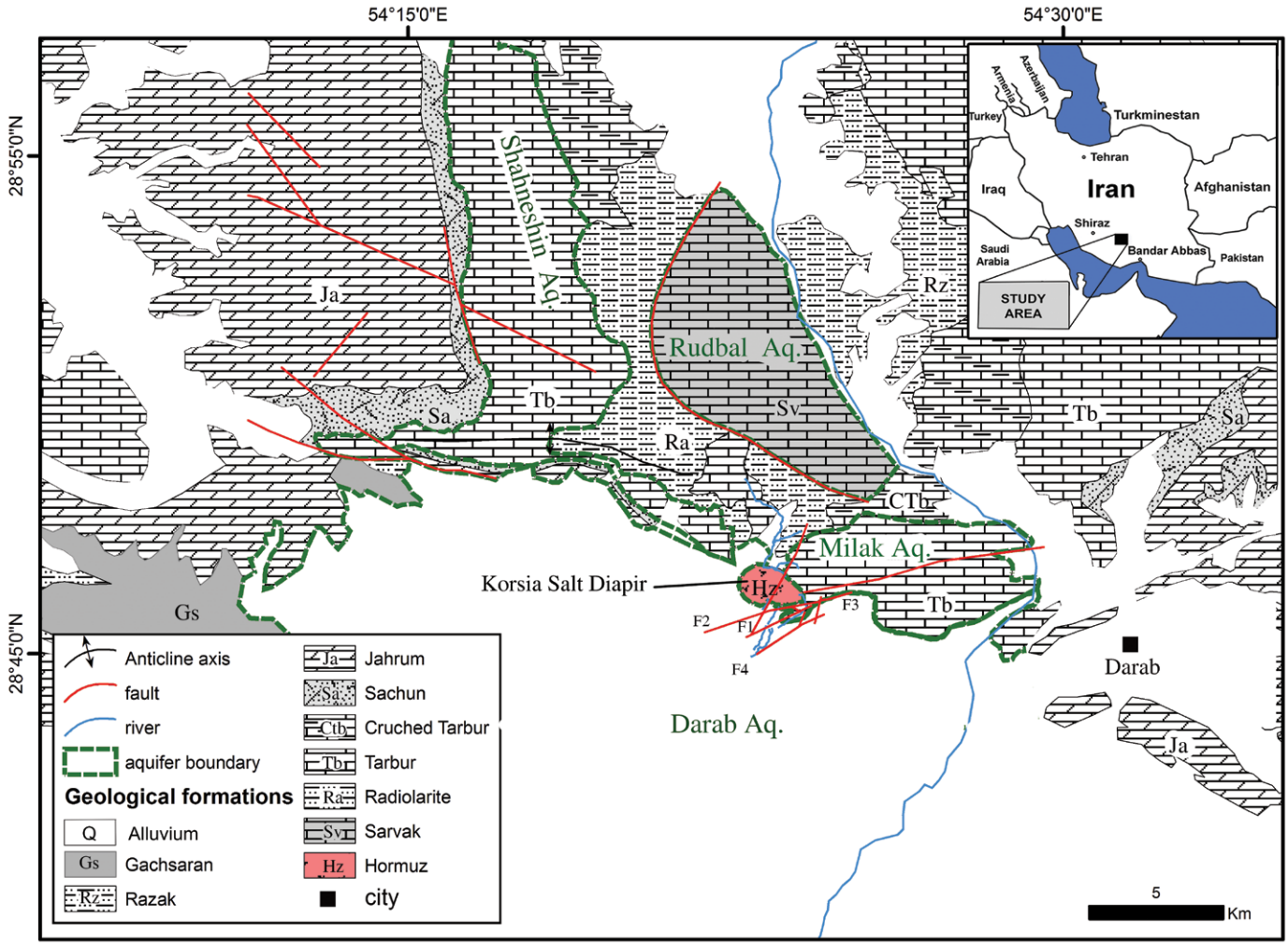

Figure 1. Geological map of the study area.

1300 meters above sea level (m.a.s.l.) and 200 m above the surrounding plain, which is located in the western section.

The diapir can be separated into two different morphological portions: i) summit and ii) low land zones (Fig. 2). The western portion, with high relief, comprises the top of the diapir (summit zone), whereas the eastern one has a low and hummocky morphology (low land zone) and is highly dissected by several faults. In the summit zone, salt is covered by residual soil, while in the low-land, it is mostly exposed.

The study area is located in a semi-arid region with a mean annual precipitation of 360 mm (Alemansour, 2015) that takes place mainly during late fall and winter. The salt diapir of Korsia is surrounded by four aquifers (Fig. 1):

Milak karst aquifer: it is located east of the diapir (Fig. 1). The aquifer is composed of well-karstified limestones of the Tarbur Formation and is in direct contact with the Korsia diapir. Milak karst aquifer discharges about 800 L/s of groundwater through two springs (S8: Korsia, and S9: Shahijan) with electrical conductivities of 2.25 and 0.44 mS/cm, respectively. They have become dry during recent years (Fig. 3a). The northern and eastern boundaries of Milak aquifer are mainly bordered by the Rudbal River.

Shahneshin karst aquifer: as for the Milak karst aquifer, it is associated with the Tarbur limestones in the northwest side of the Korsia diapir (Fig.1). Shahneshin Aquifer is drained by Golabi spring (S7). The emergence point of the spring is only 1 km away from the Korsia diapir (Fig. 3). However, the spring is of bicarbonate water type with electrical conductivity of 0.60 mS/cm.

Rudbal karst aquifer: it develops in the limestone rocks of Sarvak Formation, north of the Korsia diapir (Fig. 1). The NW boundary of the Rudbal aquifer is in contact with Rudbal River. Hydraulic connectivity of the Korsia diapir with Rudbal aquifer is interrupted by the impermeable Radiolarite Unit. No evident springs discharge the Rudbal aquifer, which likely feeds the Rudbal River. Electrical conductivity in the two sampling sites of Rudbal River (R1 to R2) decreases from 0.69 mS/cm (R1) to 0.45 mS/cm (R2) along this section, which is thought to be related to input of high-quality water from Sarvak aquifer.

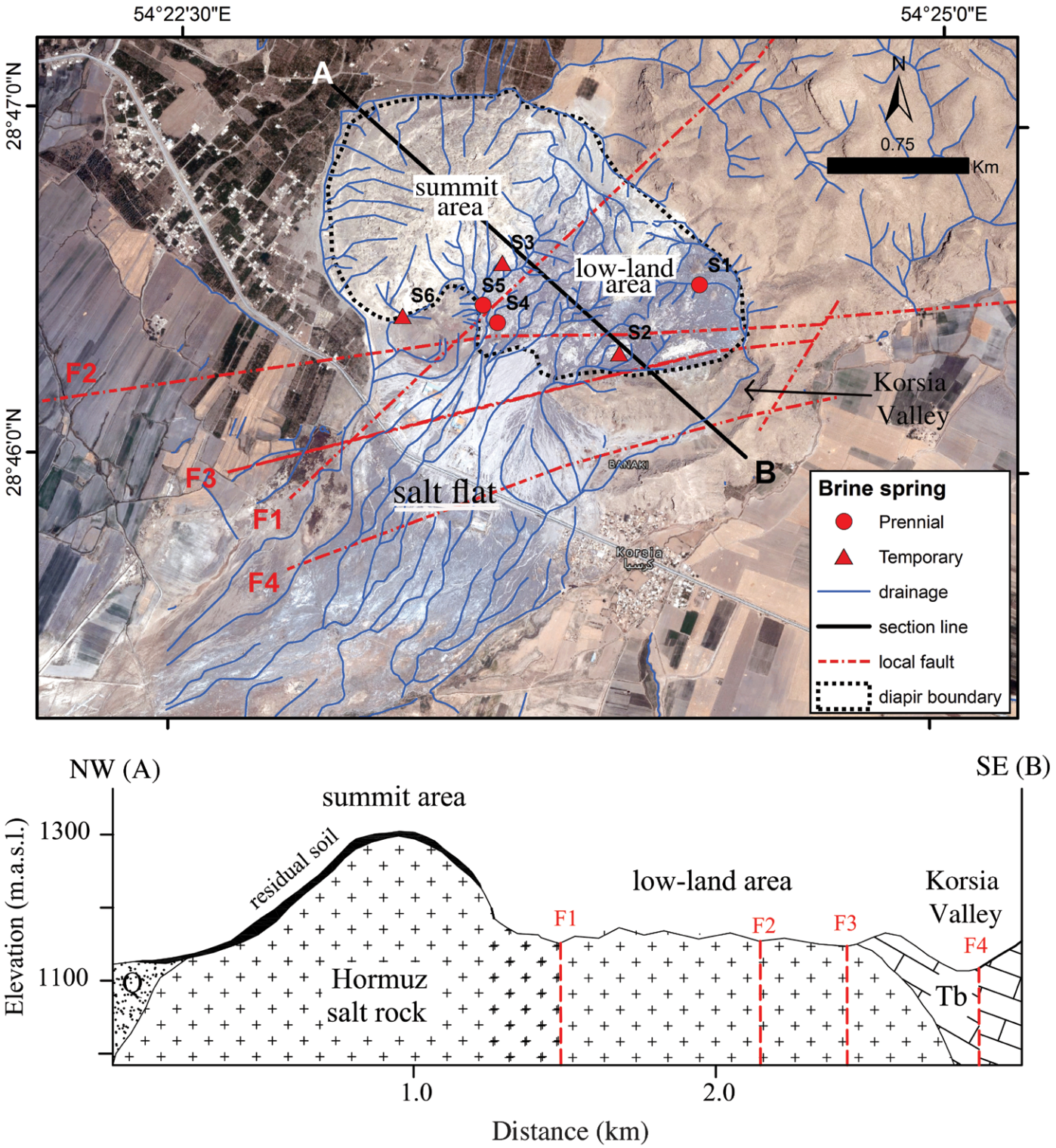

Figure 2. a) Satellite image of the study area; b) NW-SE cross-section of the Korsia salt diapir along the section line of AB.

Darab alluvial aquifer: it borders the southern and western portions of the Korsia salt diapir. In addition, the area between the Darab plain and Korsia diapir is characterized by a salt flat (Fig. 3). The electrical conductivity of groundwater in Darab plain, near the Korsia diapir, ranges from 0.40 to 5.05 mS/cm.

The Korsia salt diapir is drained by three permanent and three temporary brine springs (Fig.2a), characterized by flow rates lower than 2 L/s (Table 2). The surface runoff of the summit zone presents a radial drainage network and flows toward the surrounding Darab plain. Part of the diapir runoff and spring S1 pass through the Korsia valley,

Table 1. Morphological characteristics of the Korsia diapir[a].

Measurement	Value
Area	2.64 km^2
Perimeter	6.27 km
Maximum length	2.40 km
Maximum width	1.48 km
Maximum Elevation	1300 m.a.s.l.
Minimum Elevation	1180 m.a.s.l.

[a] Korsia diapir shape = elliptical.

which is partly in contact with limestones of the Milak karst aquifer (Figs. 2a and 2b). The spring-derived brines and saline-surface runoff from the diapir finally flow southward to the Darab plain, and this results in the development of a salt flat south of the diapir (Figs. 2 and 3).

Sampling and Analytical Methods

Electrical conductivity (EC), temperature, and pH of the 41 sampling points (Table 3) were measured in April 2013, using a portable instrument (Hach Company, model Hq40d). The sampling points include 32 exploitation wells,

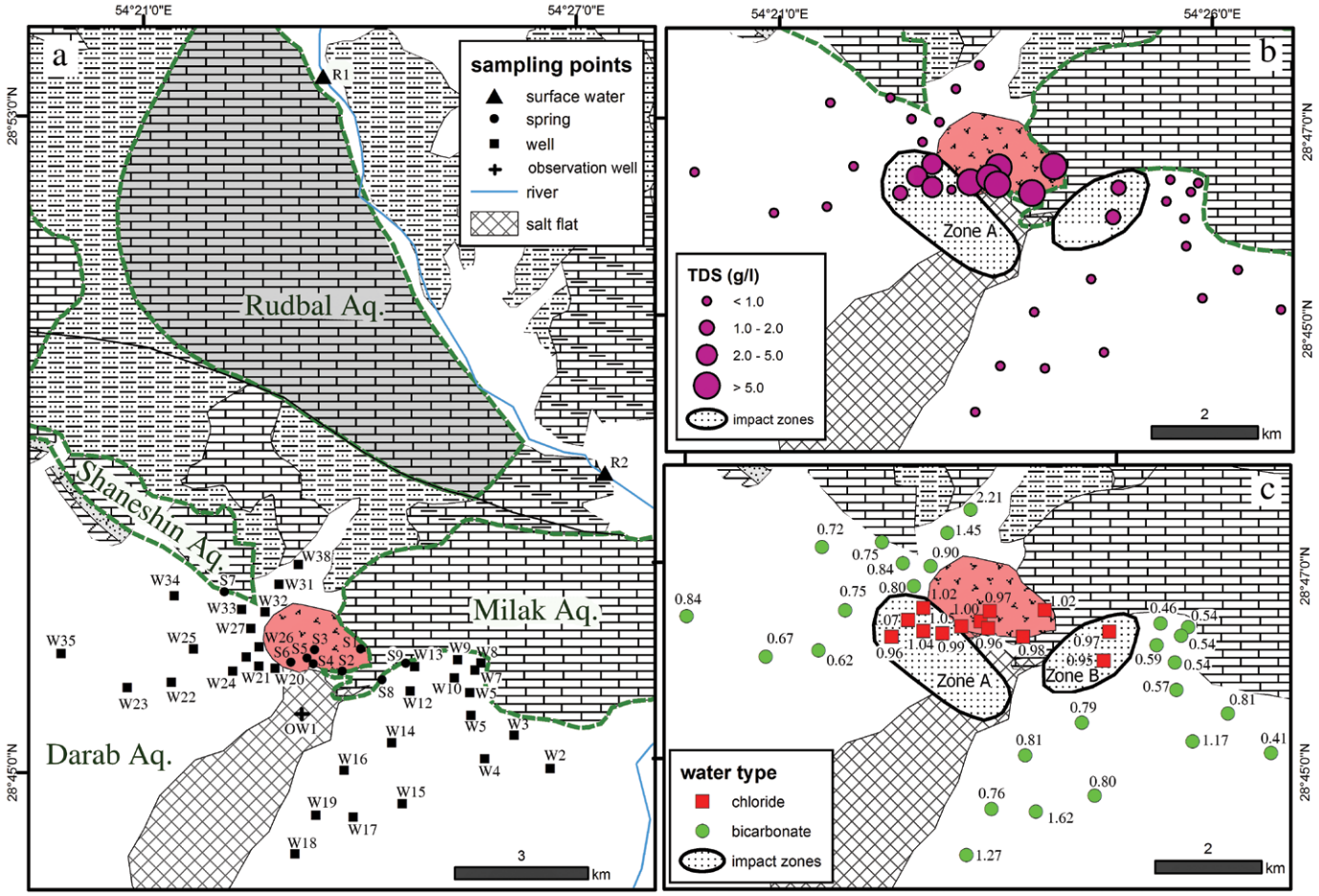

Figure 3. a) Location map of sampling points of the study area; b. distribution map of groundwater salinity (TDS: total dissolved solids); c) water type and molar ratio of Na/Cl in the study area.

Table 2. Measured parameters of the springs of the study area.

Spring Code	Spring Location	Flow Rate (L/s)	Elec. Cond. (mS/cm)	Current Status	Date of Measurement
S1	Korsia diapir	0.5	160	active	2013
S2	Korsia diapir	0.2	150	active	2013
S3	Korsia diapir	0.3	165	active	2013
S4	Korsia diapir	0.2	155	active	2013
S5	Korsia diapir	0.5	145	active	2013
S6	Korsia diapir	0.2	170	active	2013
S7 (Golabi)	Shahneshin Aq.	395	0.60	active	2013
S8 (Korsia)	Milak Aq.	430	2.25	dry	2002
S9 (Shahijan)	Milak Aq.	360	0.44	dry	2002

Table 3. List and location of sampling points.

		UTM-Zone 40N		
Sampling Location	**Source Type**	**Easting**	**Northing**	**Aquifer**
S1	Brine spring	246526	3185870	Korsia diapir
S2	Brine spring	246114	3185368	Korsia diapir
S3	Brine spring	245547	3186047	Korsia diapir
S4	Brine spring	245380	3185713	Korsia diapir
S5	Brine spring	245368	3185762	Korsia diapir
S6	Brine spring	244939	3185703	Korsia diapir
S7 (Golabi spring)	Karst spring	243437	3187289	Shahneshin aquifer
S8 (Korsia spring)	Karst spring	246982	3185317	Milak aquifer
S9 (Shahijan spring)	Karst spring	247504	3185668	Milak aquifer
W2	well	250560	3183879	East side of Darab aquifer
W3	well	250074	3183820	East side of Darab aquifer
W4	well	249603	3183760	East side of Darab aquifer
W5	well	248999	3184505	East side of Darab aquifer
W7	well	249119	3185406	East side of Darab aquifer
W8	well	249088	3185525	East side of Darab aquifer
W9	well	249222	3185688	East side of Darab aquifer
W10	well	248793	3186025	East side of Darab aquifer
W11	well	248764	3185953	East side of Darab aquifer
W12	well	247996	3185466	East side of Darab aquifer
W13	well	247712	3185715	East side of Darab aquifer
W14	well	246652	3184187	East side of Darab aquifer
W15	well	246317	3183144	East side of Darab aquifer
W16	well	246373	3182878	East side of Darab aquifer
W17	well	246197	3182452	East side of Darab aquifer
W18	well	244902	3182558	East side of Darab aquifer
W19	well	244817	3181912	East side of Darab aquifer
W20	well	244563	3185415	West side of Darab aquifer
W21	well	244411	3185748	West side of Darab aquifer
W22	well	244094	3185699	West side of Darab aquifer
W23	well	244030	3185767	West side of Darab aquifer
W2	well	243950	3186118	West side of Darab aquifer
W25	well	243836	3186132	West side of Darab aquifer
W26	well	243780	3186173	West side of Darab aquifer
W27	well	243975	3186373	West side of Darab aquifer
W28	well	244138	3186330	West side of Darab aquifer
W31	well	244669	3187460	West side of Darab aquifer
W32	well	244325	3187177	West side of Darab aquifer
W33	well	243944	3187005	West side of Darab aquifer
W34	well	242303	3187197	West side of Darab aquifer
W35	well	239751	3185896	West side of Darab aquifer
W38	well	244746	3188289	West side of Darab aquifer
R1	river	245469	3198796	Rudbal River
R2	river	246469	3196203	Rudbal River
S2	Brine spring	246114	3185368	Korsia diapir
S3	Brine spring	245547	3186047	Korsia diapir
S4	Brine spring	245380	3185713	Korsia diapir
S5	Brine spring	245368	3185762	Korsia diapir
S6	Brine spring	244939	3185703	Korsia diapir

seven springs, and two surface water stations (Fig. 3a). Water samples were taken in new, pre-rinsed polyethylene bottles to measure major- and minor-dissolved constituents.

Chemical analyses of the water samples were performed in the laboratories of the Geological Department of TU Bergakademie, Freiberg, Germany. The concentrations of major and minor ions, including calcium, magnesium, sodium, potassium, chloride, bromide, and sulfate, were determined by ion chromatography (Metrohm Compact IC Pro 881 for anions and Metrohm Professional IC 850 for cations). Bicarbonate was determined by titration with HCl, using methyl orange as indicator. Table 4 reports the results of the chemical analysis of water samples. The ion balance error did not exceed 5 % in any of the samples analyzed.

In addition, seven of the 41 samples were analyzed for stable isotopes of oxygen-18 and deuterium in the laboratories of TU Bergakademie, Freiberg, Germany. The isotopic composition ($\delta^{18}O$ and $\delta^{2}H$) of the water samples were measured with a laser-based device, Picarro L1102-I. Since all the brine samples are of Na-Cl type, the laboratory results of isotopes measurements are not expected to be affected by salinity effect (Sofer and Gat, 1972). Therefore, no specific correction was applied.

Results and Discussion

The Influence of the Diapir on the Surrounding Aquifers

The Korsia salt diapir is surrounded by three karst aquifers: Rudbal, Milak, Shahneshin, and an alluvial aquifer, Darab. We do not have sufficient data from the groundwaters of the Rudbal aquifer because there are no observable emerging springs or observation/exploitation wells in the aquifer. Therefore, the flow regime of the Rudbal aquifer has

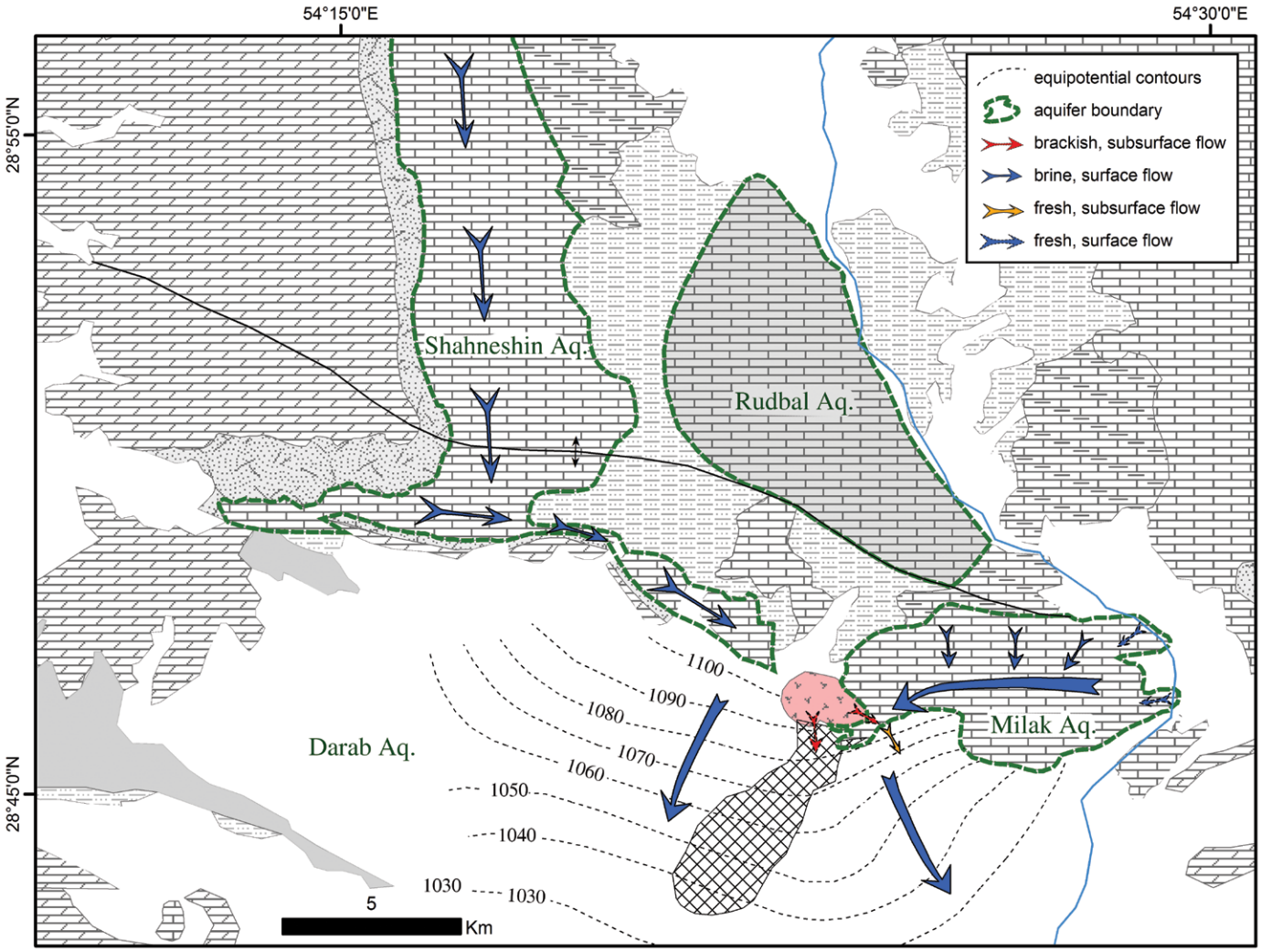

Figure 4. Conceptual groundwater flow model of the study area.

not been evaluated in the current work. However, the impact of the diapir on the karst Rudbal aquifer is unlikely, in particular, because its hydraulic connectivity is interrupted by the impermeable Radiolarite Unit.

Milak Karst Aquifer

Our observations allowed us to understand the general groundwater circulation in the Milak aquifer (Fig. 4). The main components of water recharge to the aquifer include: i) meteoric precipitation, and ii) infiltration of waters from Rudbal River. Part of the meteoric waters falling on the surface of Milak area recharge the aquifer and flow southward, following the dip direction of the strata, and then westward, parallel to the strike of limestones. In addition, the Milak aquifer receives a significant volume of water from the Rudbal River, where it flows in direct contact with the aquifer. These waters used to emerge at springs S8 and S9, located in the southwest portion of the aquifer, where the limestone crops out at the lowest elevation. The brine intrusion occurs in the western part of the aquifer, and the EC of the waters emerging at spring S8 increases from an expected value for karst waters (<0.5 to 2.25 mS/cm) (Table 2). As mentioned earlier, the springs have dried up in the last 10 years because of a severe drought in the region, and the construction of a dam in the Rudbal River, located upstream of the studied area. Perhaps, after drying out of the springs, karst waters from Milak aquifer discharge through flow to the alluvial Darab plain.

The following reasons justify the proposed water circulation model for the Milak karst aquifer:

1. The result of water balance estimation for the Milak aquifer indicates that the total outcrop area of the aquifer is not sufficient to provide flow rates of 430 and 360 L/s from the springs S8 (Korsia) and S9 (Shahijan), respectively. The annual volume of precipitation recharging the Milak aquifer is estimated using Equation (1) and information provided in Table 5.

$$V = PIA \quad (1)$$

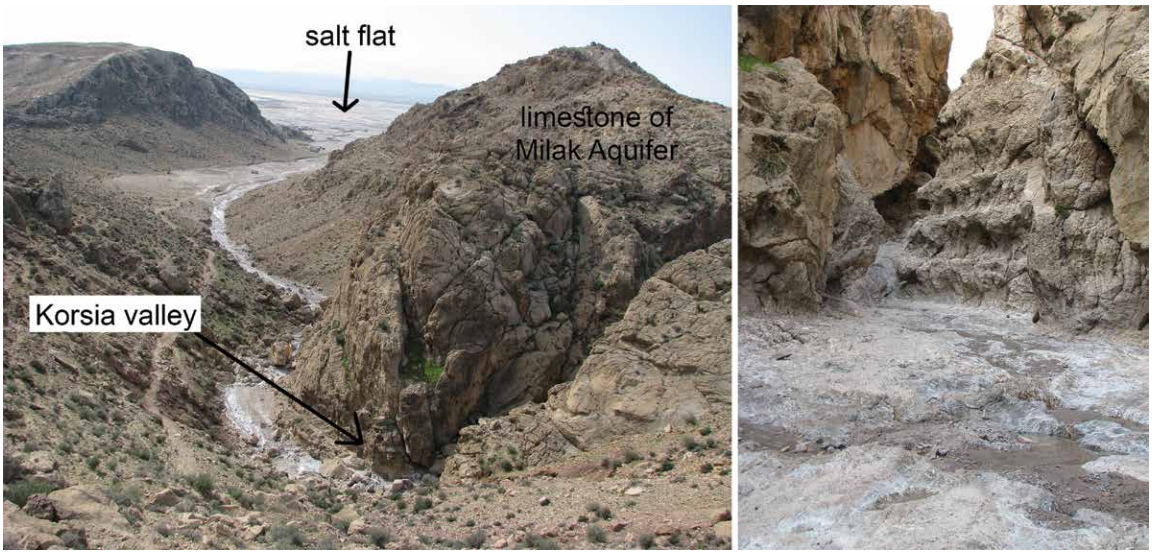

Figure 5. a) A photograph looking south showing Korsia valley located in the east of the diapir; b) flow of brine originating from spring S1, infiltrating into the limestone of Milak Aquifer on the bed of Korsia Valley.

where V is the total annual volume of recharge to the aquifer, P is the annual precipitation on the aquifer outcrop (0.340 m), I is the recharge coefficient (0.40 m), and A is the Milak aquifer outcrop area (28.7 km^2). The calculated value for the recharge volume V to the aquifer is 110 L/s, which is significantly lower than the discharge volume observed at springs S8 and S9. This suggests that there is another recharge source for the aquifer, in addition to the direct precipitation on the aquifer. Regarding the direct contact of the aquifer with the Rudbal River, seepage from the river is the most likely source of extra recharge for the Milak aquifer, especially through the Shahijan Fault (F2 on Fig. 1). A significant decrease in flow rate of the river, after dam construction, resulted in a quick lowering of water table in the Milak karst aquifer. Therefore, springs S8 and S9 dried up and karst water of the Milak aquifer discharges to the Darab alluvial plain as a subsurface flow, pointed out by the equipotential map of the Darab alluvial Plain in this area (Fig. 4).

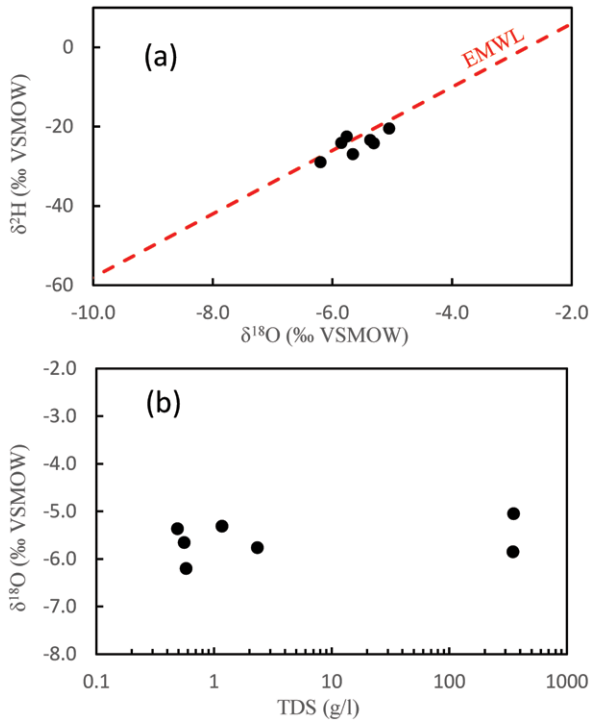

Figure 6. a) δ2H vs. δ18O diagram for water samples, EMWL: eastern Mediterranean meteoric water line; b) variation of δ18O vs. TDS (total dissolved solids) of groundwater samples.

b. Comparing the water quality of springs S8 and S9, we observed that spring S8 presents EC of 2.25 mS/cm and Na-Cl waters, mainly influenced by diapir brines, which have, on the other hand, no impact on S9 water, showing EC of 0.44 mS/cm and Ca-HCO_3 waters. A portion of the brine flows into the Milak aquifer somewhere between the emerging points of these two springs. Therefore, the part of karst water flowing westward and discharging through spring S8 receives some brine infiltrated into the aquifer. In addition, our field observations indicate that the brine infiltration into the limestone of the Milak aquifer occurs from the eastern side of the diapir. Part of the diapir-derived brine flows eastward on limestone outcrops in Korsia Valley (Fig. 2 and Fig. 5). Flowing through the valley, salt water of the brine stream infiltrates into the limestones at the valley bottom.
c. Spatial distribution of the groundwater quality in the alluvial Darab aquifer shows an increase in the salinity of the exploitation wells located in a zone, where the Milak aquifer discharges into the Darab Alluvium. The front of brine intrusion has propagated to the east during recent years. Consequently, well W13, located close to the former emerging point of spring S9, with EC of 0.44 mS/cm, has EC of 1.71 mS/cm, with a chloride water type at the present time.
d. The molar ratio of Na/Cl of groundwater samples has been plotted in Figure 3c. Investigation of ion ratios indicates that karst water discharging to Darab aquifer is influenced by diapir brine in the western sector of the discharge zone. The Na/Cl molar ratio of wells W12 and W13, located close to the diapir, are 0.95 and

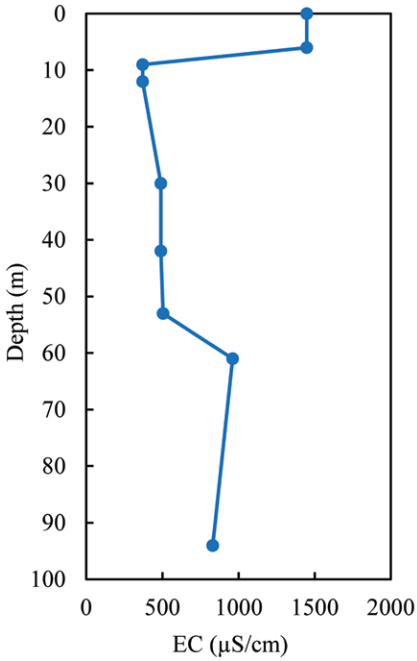

Figure 7. Variations of electrical conductivity (EC) with depth in observation well of OW1.

0.97, respectively, which are especially close to the average Na/Cl ratio of brine springs of the diapir (0.99). The ratio is lower than 0.8 in wells located further east, including W7, W8, W9, W10 and W11, which indicates no impact of diapir brine in that area (Fig. 3c). In addition, the weight ratios of Br/Cl (Table 4) are less than 4×10^{-4} in groundwater samples from W12 and W13, falling in the proposed range of Br/Cl ratio for saline water resulting from halite dissolution (Richter et al., 1991), and is also close to the ratio calculated for the brine springs of Korsia diapir (2.5×10^{-4}).

Shahneshin Karst Aquifer

Shahneshin karst aquifer is located on the west side of the Korsia salt diapir (Fig. 1). Part of the meteoric precipitation falling on the limestone outcrops recharges to the aquifer. The general flow direction in the aquifer is mainly N-S, across the axis of an anticline. Then karst water flows toward the southeast, following the strike of the limestone strata, finally emerging at Golabi Spring (S7) with a flow rate of 395 L/s, as the only discharging point of the aquifer.

The limestone of Tarbur is sandwiched between two impermeable layers. It is underlain by the Radiolarite Unit and overlain by the Sachun Formation. Therefore, discharge of karst water is only likely in the far southeast of the aquifer, where the limestone outcrops lay at the lowest elevation, and where spring S7 is located. The presence of the impermeable Sachun Formation, in the southern boundary of the aquifer, prevents subsurface discharge of karst water into the Darab alluvial aquifer.

Water budget calculations indicate that meteoric precipitation recharging to the outcrop area of the Shahneshin aquifer is sufficient to provide the karst water discharging via spring S7, with an annual volume discharge of 12.5 MCM or 395 L/s (Table 5). The annual recharge volume to the Shahneshin Aquifer is estimated at 12.6 MCM (equivalent to 400 L/s) using Equation (1), given the outcrop area of 78.05 km^2, an annual precipitation of 405 mm and a recharge coefficient of 0.40.

Golabi spring (S7) is located in the eastern sector of the Shahneshin aquifer and 1000 m away from the salt diapir. However, electrical conductivity of the spring water is 0.60 mS/cm, which is characteristic of typical fresh waters dominated by Ca-HCO_3 water type. These confirm the lack of brine intrusion from Korsia diapir into the Shahneshin aquifer.

Darab Alluvial Aquifer

Darab alluvial aquifer is located in the south side of the Korsia diapir (Fig. 1), whereas its northern part is in direct contact with Milak karst aquifer. Generally, groundwater flows from the northern toward the southern sector (Fig. 4). Therefore, recharge in the northern mountains, as surface runoff and subsurface flow, represents the main water source for the alluvial aquifer. Figure 3b indicates the spatial distribution of salinity in Darab aquifer around the Korsia Diapir and suggests two zones of high-salinity groundwater: Zone A (adjacent to the Korsia diapir) and Zone B (adjacent to the Milak aquifer). Figure 4 illustrates the general flow direction in the Darab Aquifer. The following reasons justify the proposed model:

Zone A (south of the diapir (is mainly influenced by brines emerging from springs. In addition, flow of saline surface runoff, originated from the surface of the diapir, causes additional salinization of Zone A. Infiltration of surface saline water in Zone A causes an increase in the salinity of groundwater in this zone.

Subsurface inflow of brackish water from Milak Aquifer causes an increase of groundwater salinity in Zone B (adjacent to Milak Aquifer). As mentioned earlier, part of the diapir brine flows into the western section of Milak aquifer. Then brackish karst water of Milak Aquifer flows into the alluvium of Darab Aquifer, which increases salinity of exploitation wells located in Zone B.

Generally, Darab Aquifer presents bicarbonate (HCO_3) waters, which in Zones A and B have become chloride waters because of the intrusion of diapir-derived brine.

The molar ratio of Na/Cl of groundwater samples from Zones A and B varies between 0.95 and 1.07 (Fig. 3b), which are markedly close to the average Na/Cl ratio of brine springs of the Korsia diapir (0.99). Furthermore, the ratio of Br/Cl is lower than 5×10^{-4} (Table 4) in groundwater samples of wells located in Zones A and B, which suggests that the source of salinity is salt diapir (Richter et al., 1991).

The isotopic composition of all groundwater samples was plotted on the $\delta^{18}O$-$\delta^{2}H$ diagram of Figure 6a. Since there is no local meteoric line in the study area, and meteoric precipitation mainly originated from Mediterranean air masses, the Eastern Mediterranean Meteoric Water Line (EMWL) is considered as the meteoric water line of the area. All samples plot very close to the EMWL, which shows that evaporation does not play any significant role on groundwater salin-

Table 4 Results of the chemical analysis of water sample in the study area.

Sampling Location	Water Type	Elec. Cond. (mS/cm)	TDS (g/L)	Ca (mg/L)	Mg (mg/L)	Na (mg/L)	K (mg/L)	SO_4 (mg/L)	Cl (mg/L)	HCO_3 (mg/L)	Br (mg/L)	Na/Cl (molar)	Br/Cl [× 10^{-4}] (molar)
S1	Cl	160	352	1550	349.4	138400	496.2	2260	209200	42.7	39.7	1.02	1.9
S2	Cl	150	341	1680	273.4	130900	471.1	2430	205600	48.8	···	0.98	···
S3	Cl	165	378	950.0	1220	141900	1610	5260	226900	61.0	···	0.97	···
S4	Cl	155	335	1380	683.6	127900	581.4	3130	205600	30.5	···	0.96	···
S5	Cl	145	349	2510	106.3	133900	691.6	4250	207400	30.5	70.5	1.00	3.4
S6	Cl	170	362	1300	607.6	144900	671.3	2080	212700	30.5	48.9	1.05	2.3
S7	HCO_3	0.60	0.558	76.2	23.1	25.8	1.56	64.8	53.18	305.1	0.069	0.75	13.0
W2	HCO_3	0.80	0.652	78.2	41.3	47.4	1.96	92.7	177.30	213.6	···	0.41	···
W3	HCO_3	0.72	0.709	64.1	46.2	65.1	2.35	169.6	124.10	238.0	0.434	0.81	35.0
W4	HCO_3	0.55	0.532	60.1	48.6	26.9	1.56	127.3	35.45	231.9	···	1.17	···
W5	HCO_3	0.81	0.721	82.2	43.8	67.8	1.56	103.3	184.40	238.0	···	0.57	···
W7	HCO_3	0.50	0.543	60.1	30.4	24.6	1.56	92.7	70.91	262.4	0.121	0.54	17.1
W8	HCO_3	0.54	0.518	62.1	48.6	14.9	1.17	43.7	42.54	305.1	···	0.54	···
W9	HCO_3	0.42	0.504	78.2	29.2	13.8	1.17	78.8	28.36	274.6	···	0.75	···
W10	HCO_3	0.43	0.492	74.1	26.7	12.2	1.17	101.3	31.91	244.1	···	0.59	···
W11	HCO_3	0.40	0.511	92.2	15.8	17.9	1.17	85.5	60.27	238.0	0.072	0.46	11.9
W12	Cl	1.40	1.016	134.3	64.4	214	2.35	162.3	354.50	213.6	0.106	0.95	3.0
W13	Cl	1.71	1.174	100.2	52.3	280	1.56	78.8	453.80	238.0	0.095	0.97	2.1
W14	HCO_3	0.70	0.661	90.2	45.0	67.6	2.35	96.1	131.20	268.5	0.223	0.79	17.0
W15	HCO_3	0.50	0.555	58.1	52.3	25.8	1.96	92.7	49.63	274.6	···	0.80	···
W16	HCO_3	0.72	0.670	90.2	41.3	28.1	1.96	101.3	53.18	353.9	···	0.81	···
W17	HCO_3	0.40	0.474	64.1	28.0	26.0	1.56	54.8	24.82	274.6	···	1.62	···
W18	HCO_3	0.52	0.522	40.1	42.5	46.7	1.17	47.6	56.72	286.8	0.091	1.27	16.0
W19	HCO_3	0.60	0.576	66.1	42.5	43.5	1.56	76.9	88.63	256.3	0.152	0.76	17.1
W20	Cl	5.05	0.850	100.2	48.6	1190.0	1.56	827.8	1860.00	384.4	0.279	0.99	1.5
W21	Cl	3.02	2.337	30.1	30.4	513.3	2.74	447.2	759.70	366.1	0.137	1.04	1.8
W22	HCO_3	0.80	0.694	110.2	24.3	45.3	1.96	75.4	113.4	323.4	0.261	0.62	23.0
W23	HCO_3	0.80	0.811	108.2	43.8	41.6	1.96	153.7	95.72	366.1	···	0.67	···
W24	Cl	1.90	1.275	220.4	30.4	286.3	3.13	231.1	460.90	292.9	0.23	0.96	5.0
W25	HCO_3	0.70	0.653	90.2	32.8	36.3	1.56	131.1	74.45	286.8	···	0.75	···
W26	Cl	3.10	2.381	116.2	51.0	579.6	1.96	482.2	833.10	317.3	···	1.07	···
W27	HCO_3	0.60	0.595	84.2	42.5	31.3	1.17	101.3	60.27	274.6	116	0.80	19.2
W28	Cl	4.40	2.643	78.2	28.0	820	4.30	172.9	1241.00	299.0	0.397	1.02	3.2
W31	HCO_3	1.03	0.955	90.2	48.6	133.3	2.35	148.4	141.80	390.5	···	1.45	···
W32	HCO_3	0.90	0.791	96.2	45.0	64.4	1.96	138.3	109.90	335.6	0.165	0.90	15.0
W33	HCO_3	0.62	0.638	70.1	41.3	36.8	3.91	101.3	67.36	317.3	···	0.84	···
W34	HCO_3	0.40	0.508	66.1	35.2	19.8	1.56	92.7	42.54	250.2	···	0.72	···
W35	HCO_3	0.90	0.777	110.2	42.5	53.8	2.35	113.8	99.63	366.1	···	0.84	···
W38	HCO_3	0.90	0.571	44.1	28.0	86.2	1.96	75.4	60.27	274.6	···	2.22	···
R1	HCO_3	0.69	0.875	125.1	50.7	25.3	2.30	145.1	49.36	336.8	0.095	0.79	19.2
R2	HCO_3	0.45	0.530	84.2	29.2	17.0	1.17	83.1	28.36	286.8	···	0.93	···

Table 5. Water balance parameters of Milak and Shahneshin Aquifers.

Parameter	Milak	Shahneshin
Outcrop area (km^2)	78.05	28.70
Annual precipitation (mm)	405	340
Recharge coefficient (%)	40	40
Calculated recharge (Mm^3)	12.6	3.5
Aquifer discharge through springs (Mm^3)	12.5	24.9

Table 6. Results of analysis of stable isotope in selected water samples.

Sample	VSMOW		Elec. Cond. (mS/cm)
	δ^2H, %	$\delta^{18}O$, %	
S1	−20.4	−5.1	352.3
S5	−24.1	−5.9	348.9
S7	−27.0	−5.7	0.56
W19	−28.9	−6.2	0.58
W21	−22.5	−5.8	2.34
W13	−24.2	−5.3	1.17
W10	−23.3	−5.4	0.49

ity of the water samples. Additionally, this is confirmed by Figure 6b, which shows no enrichment of $\delta^{18}O$ with increasing salinity.

A salt flat has been developed south of the diapir, in Zone A. Field observations show (Figs. 2 and 5) flow of direct runoff and discharge of brine springs toward the surface of Darab Aquifer in Zone A. In addition, the satellite image in Figure 2 indicates that there is no cultivation south of the Korsia diapir, which justifies low quality of groundwater and soil in Zone A, while agricultural activities in the west of the diapir indicates no impact of the diapir on this area.

A monitoring well was drilled in the south of the diapir by Water Authority of Fars Province (Well OW1 in Fig. 3a). Figure 7 illustrates the results of measurement of electrical conductivity with depth in this well. A general declining trend of salinity with depth is observed, which suggests that Zone A is influenced by brine mainly flowing in the upper portion of the Darab aquifer.

Conclusion

Fragility of the karst environment determines high possibility for pollution's rapid transport within karst conduits (Allshorn et al., 2007; Ford and Williams, 2007), with serious problems in recovering a contaminated aquifer to its pre-contamination state (Milanovic, 1981; Kacaroglu, 1999; Stevanovic et al., 2010; Parise et al. 2015, 2018). In Iran, more than 50 % of salt diapirs in the southern part of the country deteriorate water quality of the surrounding aquifers (Zarei, 2016). Located in the south-central Iran, Korsia salt diapir is surrounded by alluvial and karst aquifers. Our investigations indicate that the Korsia diapir influences the eastern karst aquifer (Milak Aquifer) and the southern alluvial aquifer (Darab Aquifer), whereas it has no impact on the western karst aquifer of Shahneshin. Infiltration of brine emerging from a spring in the east of the Korsia diapir leads to an increase of up to 2.25 mS/cm in the salinity of karst waters in the western part of Milak aquifer. The westward flow direction of karst water in the Milak Aquifer prevents flow of saline water to the eastern section of the aquifer. However, a decline in the recharge rate of the aquifer, subsequent to the construction of a dam on the Rudbal River, caused an eastward advance of the salinity front in recent years. Thereafter, salt karst water in the west of the Milak Aquifer discharges as subsurface flow toward the adjoining alluvium of Darab Aquifer, deteriorating the quality of the aquifer in this zone. Conveying brine from perennial spring S1 to salt-evaporation basins would improve water quality of the karst aquifer and would result in economic benefits by producing salt for local and industrial uses after the required treatments. The Darab Aquifer is also influenced by infiltration of saline surface runoff from the diapir and brine emerging via springs around the diaper that drain southward to the alluvium of the Darab Aquifer. Construction of salt evaporation basins could be used to collect surface saline waters originating from the diapir. This would prevent infiltration of brine into the ground and would increase the quality of the groundwater and soil of the alluvial aquifer. The karst waters coming from Shahneshin Aquifer and emerging in Golabi Spring (S7), located less than 1 km away from the west of Korsia salt diapir, show high quality. The salt diapir has no impact on water quality of the Shahneshin Aquifer due to the presence of the impermeable Radiolarite Unit that interrupts the hydraulic connectivity of the diapir with the Shahneshin karst aquifer.

Acknowledgments

This research was financially supported by Fars Regional Water Authority. The authors are indebted to Prof. Francisco Gutierrez for the improvement of English language in the manuscript.

References

Abirifard, M., Raesi, E., Zarei, M., Zare, M., Filippi, M., Bruthans, J., Talbot, Ch. J., 2017, Jahani salt diapir, Iran: hydrogeology, karst features and effect on surroundings environment, International Journal of Speleology, v. 46, no. 3, p. 445–457. https://doi.org/10.5038/1827-806X.46.3.2133.

Alavi, M., 2004, Regional stratigraphy of the Zagros fold-thrust belt of Iran and its proforeland evolution, American Journal of Science, v. 304, no. 1, p. 1–20. https://doi.org/10.2475/ajs.304.1.1.

Alemansour, Z., 2015, Investigating the effect of Korsia salt diapir on the adjacent water resources [MSc. Dissertation]: Shiraz, Iran, Department of Earth Sciences, Shiraz University. p. 345.

Allshorn, S.J.L., Bottrell, S.H., West, L.J., Odling, N.E., 2007, Rapid karstic bypass flow in the unsaturated zone of the Yorkshire chalk aquifer and implications for contaminant transport, *in* Parise, M., Gunn, J. eds., Natural and anthropogenic hazards in karst areas: recognition, analysis and mitigation, Geological Society, London, vol. 279, p. 111–122. https://doi.org/10.1144/SP279.10.

Anderson, N.L., and Brown, R.J., 1992, Dissolution and deformation of rock salt, Stettler area, Southeastern Alberta, Canadian Journal of Exploration Geophysics, v. 28, no. 2, p. 128–136.

Berberian, M., and King, G.C.P., 1981, Towards a paleogeography and tectonic evolution of Iran, Canadian Journal of Earth Sciences, v. 18, no. 2, p. 210–265. https://doi.org/10.1139/e81-019.

Yiang Bo., Liu Chenglin, Jiao Pengcheng, Chen Yongzhi, and Cao Yangtong, 2013, Hydrochemical characteristics and controlling factors for waters' chemical composition in the Tarim Basin, Western China, Chemie der Erde-Geochemistry, v. 73, no. 3, p. 343–356. https://doi.org/10.1016/j.chemer.2013.06.003.

Bosák, P., Bruthans, J., Filippi, M., Svoboda, T., and Šmíd, J., 1999, Karst and caves in salt diapirs, SE Zagros Mts. (Iran), Acta Carsologica, v. 28, p. 41–75.

Bruthans, J., Šmíd, J., Filippi, M., Zeman, O., 2000, Thickness of caprock and other important factors affecting morphogenesis of salt karst, Acta Carsologica, v. 29, no. 2, p. 51–64.

Bruthans, J., Filippi, M., Geršl, M., Zare, M., Melková, J., Pazdur, A., Bosák, P., 2006, Holocene marine terraces on two salt diapirs in Persian Gulf (Iran): age, depositional history and uplift rates, Journal of Quaternary Science, v. 21, no. 8, p. 843–857. https://doi.org/10.1002/jqs.1007

Bruthans, J., Asadi, N., Filippi, M., Vilhelm, Z., Zare, M., 2008, Erosion rates of salt diapirs surfaces: An important factor for development of morphology of salt diapirs and environmental consequences (Zagros Mts., SE Iran), Environmental Geology, v. 53, no. 5, p. 1091–1098.

Bruthans, J., Filippi, M., Asadi, N., Zare, M., Šlechta, S., Churáčková, Z., 2009, Surficial deposits on salt diapirs (Zagros Mts. and Persian Gulf Platform, Iran): Characterization, evolution, erosion and influence on landscape morphology, Geomorphology, v. 107, p. 195–209. https://doi.org/10.1016/j.geomorph.2008.12.006.

Bruthans, J., Filippi, M., Zare, M., Churáčková, Z., Asadi, N., Fuchs, M., Adamovič, J., 2010, Evolution of salt diapir and karst morphology during the last glacial cycle: effects of sea-level oscillation, diapir and regional uplift, and erosion (Persian Gulf, Iran), Geomorphology, v. 121, p. 291–304. https://doi.org/10.1016/j.geomorph.2010.04.026.

Bruthans, J., Kamas, J., Filippi, M., Zare, M., Mayo, A.L., 2017, Hydrology and chemical/isotopic composition of salt karst waters under different cap soils and climate (Persian Gulf and Zagros Mts., Iran), International Journal of Speleology, v. 46, no. 2, p. 303–320. https://doi.org/10.5038/1827-806X.46.2.2109.

Cartwright, I., Weaver, T.R., and Fifield, L.K., 2006, Cl/Br ratios and environmental isotopes as indicators of recharge variability and groundwater flow: an example from the southeast Murray Basin, Australia, Chemical Geology, v. 231, no. 1–2, p. 38–56. https://doi.org/10.1016/j.chemgeo.2005.12.009.

Charef, A., Ayed, L., and Azzouzi, R., 2012, Impact of natural and human processes on the hydrochemical evolution of overexploited coastal groundwater: case study of the Mornag aquifer refill (South-East Tunis, Tunisia), Chemie der Erde-Geochemistry, v. 72, no. 1, p. 61–69. https://doi.org/10.1016/j.chemer.2011.11.005.

Chiesi, M., De Waele, J., and Forti, P., 2010, Origin and evolution of a salty gypsum/anhydrite karst spring: the case of Poiano (Northern Apennines, Italy), Hydrogeology Journal, v. 18, no. 5, p. 1111–1124. https://doi.org/10.1007/s10040-010-0576-2.

Davidson, S.C., and Mace, R.E., 2006, Aquifers of the Gulf Coast of Texas: an overview. Aquifers of the Gulf Coast of Texas, Texas Water Development Board, Austin, p. 1–22.

De Waele, J., Piccini, L., Columbu, A., Madonia, G., Vattano, M., Calligaris, C., D'Angeli, I.M., Parise, M., Chiesi, M., Sivelli, M., Vigna, B., Zini, L., Chiarini, V., Sauro, F., Drysdale, R. and Forti, P., 2017, Evaporite karst in Italy: a review, International Journal of Speleology, v. 46, no. 2, p. 137–168. https://doi.org/10.5038/1827-806X.46.2.2107.

Ebrahimi, M., Kazemi, H., Ehtashemi, M., and Rockaway, T.D., 2016, Assessment of groundwater quantity and quality and saltwater intrusion in the Damghan Basin, Iran, Chemie der Erde-Geochemistry, v. 76, no. 2, p. 227–241. https://doi.org/10.1016/j.chemer.2016.04.003.

Falcon, N.L., 1967, The geology of the north-east margin of the Arabian basement shield, Advancement of Science, v. 24, p. 31–42.

Falcon, N.L., 1974, Southern Iran: Zagros Mountains, Geological Society, London, Special Publications, v. 4, p. 199–211. https://doi.org/10.1144/GSL.SP.2005.004.01.11.

Ford, D.C., Williams, P., 2007, Karst hydrogeology and geomorphology. Wiley, Chichester. https://doi.org/10.1002/9781118684986.

Frumkin, A., 1994, Hydrology and denudation rates of halite karst, Journal of Hydrology, v. 162, no. 1–2, p. 171–189. https://doi.org/10.1016/0022-1694(94)90010-8.

Frumkin, A., 2000, Speleogenesis in salt–The Mount Sedam area, Israel, *in* Klimchouk, A.V., Ford, D.C., Palmer, A.N., Dreybrodt, W. eds., Speleogenesis; Evolution of karst aquifers, k, Huntsville, Alabama, National Speleological Society, p. 443–451.

FDA, 2016, Electronic Code of Federal Regulations, in U.F.A.D., eds., Administration, p. 606.

Hamlin, H.S., 2006, Salt domes in the Gulf Coast aquifer, *in* Aquifers of the Gulf Coast of Texas, Mace, R.E., Davidson, S.C., Angle, E.S., and Mullican, W.F., eds., Texas Water Development Board, Report, no. R365, p. 217–230.

James, G., and Wynd, J., 1965, Stratigraphic nomenclature of Iranian oil consortium agreement area, AAPG Bulletin, v. 49, p. 2182–2245.

Jirsa, F., Gruber, M., Stojanovic, A., Omondi, S.O., Mader, D., Körner, W., and Schagerl, M., 2013, Major and trace element geochemistry of Lake Bogoria and Lake Nakuru, Kenya, during extreme draught, Chemie der Erde-Geochemistry, v. 73, no. 3, p. 275–282. https://doi.org/10.1016/j.chemer.2012.09.001.

Kacaroglu, F., 1999, Review of groundwater pollution and protection in karst areas, Water, Air, and Soil Pollution, v.. 113, no. 1–4, p. 337–356. https://doi.org/10.1023/A:1005014532330.

Karimi, H., and Taheri, K., 2010, Hazards and mechanism of sinkholes on Kaboudar Ahang and Famenin plains of Hamadan, Iran, Natural Hazards, v. 55, no. 2, p. 481–499. https://doi.org/10.1007/s11069-010-9541-6

Kent, P., 1979, The emergent Hormuz salt plugs of southern Iran, Journal of petroleum geology, v. 2, p. 117–144. https://doi.org/10.1111/j.1747-5457.1979.tb00698.x.

Kharroubi, A., Tlahigue, F., Agoubi, B., Azri, C., and Bouri, S., 2012, Hydrochemical and statistical studies of the groundwater salinization in Mediterranean arid zones: case of the Jerba coastal aquifer in southeast Tunisia, Environmental Earth Sciences, v. 67, p. 2089–2100. https://doi.org/10.1016/S0016-7037(01)00640-8.

Kloppmann, W., Négrel, P., Casanova, J., Klinge, H., Schelkes, K., and Guerrot, C., 2001, Halite dissolution derived brines in the vicinity of a Permian salt dome (N German Basin). Evidence from boron, strontium, oxygen, and hydrogen isotopes, Geochimica et Cosmochimica Acta, v. 65, p. 4087–4101. https://doi.org/10.1016/S0016-7037(01)00640-8.

Kreitler, C.W., 1993, Geochemical techniques for identifying sources of ground-water salinization, CRC press.

Kreitler, C., and Richter, B., 1986, Hydrochemical characterization of saline aquifers of the Texas Gulf Coast used for the disposal of industrial waste, Report to the U.S. Environmental Protection Agency under Cooperative Agreement, no. CR821786-01-0, University of Texas at Austin, Bureau of Economic Geology.

Kumar, P.S., 2014, Evolution of groundwater chemistry in and around Vaniyambadi industrial area: differentiating the natural and anthropogenic sources of contamination, Chemie der Erde-Geochemistry, v. 74, no. 4, p.641–651. https://doi.org/10.1016/j.chemer.2014.02.002.

Leonard, A., and Ward, P., 1962, Use of Na/Cl ratios to distinguish oil-field from salt-spring brines in western Oklahoma, U.S. Geological Survey Professional Paper 450-B, p. 8126–8127.

Lucha, P., Cardona, F., Gutiérrez, F., and Guerrero, J., 2008, Natural and human-induced dissolution and subsidence processes in the salt outcrop of the Cardona Diapir (NE Spain), Environmental Geology, v. 53, no. 5, p.1023–1035. https://doi.org/10.1007/s00254-007-0729-3.

Lichun Ma, Qingfeng Tang, Baoguo Li, Yufei Hu, and Wenjun Shang, 2016, Sediment characteristics and mineralogy of salt mounds linked to underground spring activity in the Lop Nor playa, Western China, Chemie der Erde-Geochemistry, v. 76, no. 3, p. 383–390. https://doi.org/10.1016/j.chemer.2016.08.001.

Mehdizadeh, R., Zarei, M., and Raeisi, E., 2015, How subaerial salt extrusions influence water quality in adjacent aquifers, Journal of Hydrology, v. 531, p. 1108–1113. https://doi.org/10.1016/j.jhydrol.2015.11.021.

Milanovic, P.T., 1981, Karst hydrogeology. Water Resources Publishing, Beograd, Serbia.

Morton, A.B., 1986, Effects of brine on the chemical quality of water in parts of Creek, Lincoln, Okfuskee, Payne, Pottawatomie, and Seminole Counties, Oklahoma, U.S. Geological Survey Open-File Report 84-445, p. 37. https://doi.org/10.3133/ofr84445.

Nekouei, E., and Zarei, M., 2016, Karst hydrogeology of Karmustadj salt diapir, southern Iran, Carbonates and Evaporites, v. 32, no. 3, p. 315–323. https://doi.org/10.1007/s13146-016-0298-1.

Nekouei, E., Zarei, M., & Raeisi, E., 2016, The influence of diapir brine on groundwater quality of surrounding aquifers, Larestan, Iran, Environmental Earth Sciences, v. 75, no. 7, p. 571. https://doi.org/10.1007/s12665-015-5237-2.

Parise, M., Ravbar, N., Z˘ivanovic, V., Mikszewski, A., Kresic, N., Ma´dl-Szo¨nyi, J., Kukuric, N., 2015, Hazards in karst and managing water resources quality, *in* Stevanovic Z., ed., Karst aquifers–characterization and engineering, Professional Practice in Earth Sciences, Springer, p. 601–687. https://doi.org/10.1007/978-3-319-12850-4_17.

Parise, M., Gabrovsek, F., Kaufmann, G., and Ravbar, N., 2018, Recent advances in karst research: from theory to fieldwork and applications, *in* Parise, M., Gabrovsek, F., Kaufmann, G. and Ravbar, N., eds., Advances in Karst Research: Theory, Fieldwork and Applications, London, Geological Society, Special Publications, vol. 466, p. 1–24, https://doi.org/10.1144/SP466.26.

Richter, B.C., Dutton, A.R., and Kreitler, C.W., 1990, Identification of sources and mechanisms of salt-water pollution affecting ground-water quality: A case study, west Texas, Bureau of Economic Geology, no. RI0191D, University of Texas at Austin. https://doi.org/10.23867/RI0191D.

Richter, B.C., Kreitler, C.W., and Bledsoe, B.E., 1991, Identification of sources of ground-water salinization using geochemical techniques, U.S. Environmental Protection Agency, Report no. EPA/600/S2-91/064, Office of Research and Development, Robert S. Kerr Environmental Research Laboratory.

Salameh, E., Alraggad, M., and Tarawneh, A., 2014, Natural salinity sources in the groundwaters of Jordan–importance of sustainable aquifer management, Chemie der Erde-Gochemistry, v. 74, n. 4, p. 735–747. https://doi.org/10.1016/j.chemer.2014.04.007.

Sharafi, A., Raeisi, E., and Farhoodi, G., 1996, Contamination of the Konar Siah karst spring by salt dome, International Journal of Engineering, v. 9, p. 37–44.

Sharafi, A., Raeisi, E., and Farhoodi, G., 2002, The effect of Darab salt dome on the quality of adjacent karstic and alluvium aquifers (south of Iran), Acta Carsologica, v. 31, p. 105–113.

Sofer, Z., and Gat, J., 1972, Activities and concentrations of oxygen-18 in concentrated aqueous salt solutions: analytical and geophysical implications, Earth and Planetary Science Letters, v. 15, p. 232–238. https://doi.org/10.1016/0012-821X(72)90168-9.

Stevanovic, Z., Milanovic, S., Ristic, V., 2010, Supportive methods for assessing effective porosity and regulating karst aquifers, Acta Carsologica, vol. 39, no. 2, p. 313–329. https://doi.org/10.3986/ac.v39i2.102.

Stöcklin, J., 1968, Salt deposits of the Middle East, Geological of Society America, Special Paper SPE88, p. 157–181. https://doi.org/10.1130/SPE88-p157.

Talbot, C., and Alavi, M., 1996, The past of a future syntaxis across the Zagros, London, Geological Society, Special Publications 100, p. 89–109. https://doi.org/10.1144/GSL.SP.1996.100.01.08

Taheri, K., Taheri, M. and Parise, M., 2016, Impact of intensive groundwater exploitation on an unprotected covered karst aquifer: a case study in Kermanshah Province, western Iran, Environmental Earth Sciences, vol. 75, no. 17, p. 1221, https://doi.org/10.1007/s12665-016-5995-5.

Taheri, K., Taheri, M., Gutieŕrez, F., Safari-Komail, M., 2017, Sin-DRASTIC: a modified vulnerability mapping method for alluvial aquifer hosted by karst in the north of Hamadan province, west of Iran, *in* Proceedings EUROKARST 2016, Switzerland, Universities of Neuchatel. https://doi.org/10.1007/978-3-319-45465-8_25.

Whittemore, D.O., and Pollock, L.M., 1979, Determination of salinity sources in water resources of Kansas by minor alkali metal and halide chemistry: Kansas Water Resources Research Institute, U.S. Department of the Interior, Washington, D.C, p. 37.

Zarei, M., 2010, Hydrogeology of salt diapirs in the south of Iran [Ph.D. dissertation]: Shiraz, Iran, Department of Earth Sciences, Shiraz University.

Zarei, M., 2016, Factors governing the impact of emerged salt diapirs on water resources, Groundwater, v. 54, no. 3, p. 354–362. https://doi.org/10.1111/gwat.12370.

Zarei, M., and Raeisi, E., 2010, Conceptual modelling of brine flow into aquifers adjacent to the Konarsiah salt diapir, Cave and Karst Science, v. 37, p. 37–44.

Zarei, M., Raeisi, E., and Mahmoudi, K., 2014, The impact of salt diapirs on the quality of carbonate karst waters, Bastak, Iran, Environmental Earth Sciences, v. 71, p. 3893–3906. https://doi.org/10.1007/s12665-013-2775-3.

Zarei, M., Sedehi, F., and Raeisi, E., 2014, Hydrogeochemical characterization of major factors affecting the quality of groundwater in southern Iran, Janah Plain, Chemie der Erde-Geochemistry, v. 74, no. 4, p. 671–680. https://doi.org/10.1007/s12665-013-2775-3.

Zarei, M., Raeisi, E., Merkel, B.J., and Kummer, N. A., 2013, Identifying sources of salinization using hydrochemical and isotopic techniques, Konarsiah, Iran, Environmental Earth Sciences, v. 70, p. 587–604. https://doi.org/10.1007/s12665-012-2143-8.